



# Modification of small-crystal titanium silicalite-1 with organic bases: Recrystallization and catalytic properties in the hydroxylation of phenol



Yi Zuo, Wancang Song, Chengyi Dai, Yingping He, Mengli Wang, Xiangsheng Wang, Xinwen Guo\*

State Key Laboratory of Fine Chemicals, Department of Catalysis Chemistry and Engineering, School of Chemical Engineering, Dalian University of Technology, Dalian 116024, PR China

## ARTICLE INFO

### Article history:

Received 29 October 2012

Received in revised form

20 December 2012

Accepted 21 December 2012

Available online xxx

### Keywords:

Titanium silicalite-1

Organic base

Recrystallization

Hydroxylation of phenol

Modification

## ABSTRACT

Small-crystal titanium silicalite-1 (TS-1) with a crystal size of about 600 nm × 400 nm × 250 nm, was treated with different organic bases, including ethylamine, diethylamine, tetramethyl ammonium hydroxide, tetrapropyl ammonium hydroxide and tetrabutyl ammonium hydroxide. The treated TS-1 was characterized by X-ray powder diffraction (XRD), Fourier-transform infrared spectrum (FTIR), ultraviolet–visible diffuse reflectance spectrum (UV–vis), X-ray photoelectron spectrum (XPS), *n*-hexane and cyclohexane physical adsorption, nitrogen physisorption, inductive coupled plasma emission (ICP), scanning electron microscopy (SEM) and transmission electron microscopy (TEM). Modification with different bases led to different molar ratios of Si/Ti on the external surface, according to the XPS data. The TEM images showed that many irregular hollows were generated during modification, due to the random dissolution of framework silicon and titanium. The dissolved amorphous silica and titania recrystallize on the external surface of the TS-1 crystals in the presence of template, and different axis-oriented recrystallization occurred for different templates. Tetrapropyl ammonium favored *a*-orientation and tetrabutyl ammonium favored *b*-orientation. Especially the modification with tetrapropyl ammonium hydroxide improved the catalytic properties of small-crystal TS-1 for the hydroxylation of phenol. The conversion of phenol reached 32.6% over small-crystal TS-1 modified with 0.06 mol/L tetrapropyl ammonium hydroxide for 72 h.

© 2013 Elsevier B.V. All rights reserved.

## 1. Introduction

Since TS-1 was invented by Taramasso et al. [1], it has attracted much attention, because of its unique catalytic oxidation properties with hydrogen peroxide, such as the oxidation of alkanes [2], the epoxidation of alkenes [3], the hydroxylation of aromatics [4] and the ammoxidation of ketones [5]. The catalytic properties of TS-1 for reactions of smaller molecules (such as epoxidation of propene) are excellent, but for reactions of larger molecules (such as the hydroxylation of phenol) they were inadequate, due to the diffusion limitation by the size of the channels (0.56 nm × 0.53 nm) [6]. Therefore, many studies focused on the improvement of the pore structure of TS-1 [7] and the exploration of titanium-containing mesoporous molecular sieves [8].

Benzenediols (catechol and hydroquinone) are important intermediates used in spices, dyes, medicines and pesticides [9]. The

traditional Rhone-Poulenc and Brichima routes for benzenediol manufacture, using strong acid or base as the catalyst, produced much pollution and corroded the equipment seriously [10]. Hydroxylation of phenol with hydrogen peroxide over TS-1, which was first commercialized by Enichem in 1986 [11], was an alternative environmental friendly route, using methanol and acetone as the solvents at 353 K. The conversion of phenol could reach 25% in the Enichem route, which was much higher than the conversions reached in the Rhone-Poulenc route (5%) and Brichima route (10%). However, many problems still exist, such as the short lifetime and low output of the catalyst.

Tetrahedrally coordinated Ti (usually called framework Ti) is considered as the active center for the hydroxylation of phenol [12], while anatase TiO<sub>2</sub> would cause the decomposition of H<sub>2</sub>O<sub>2</sub> [13]. Thus, researchers tried to increase the content of titanium in the framework. However, titanium cannot be inserted into the framework unlimitedly, due to the expansion of the lattice [14]. The maximum amount of titanium that can be introduced in the framework by hydrothermal synthesis was reported to be 2.5 wt% [15]. If the amount of titanium exceeds 2.5 wt%, it must exist as

\* Corresponding author. Tel.: +86 411 84986133; fax: +86 411 84986134.  
E-mail address: [guoxw@dlut.edu.cn](mailto:guoxw@dlut.edu.cn) (X. Guo).

extra-framework Ti. Fan et al. obtained TS-1 free of extra-framework Ti by adding ammonium salts such as  $(\text{NH}_4)_2\text{CO}_3$  in the hydrothermal synthesis [16], but the amount of framework Ti was still less than the maximum. The gas–solid synthesis of Ti-ZSM-5, using the precursor of dealuminated ZSM-5 [17] or deboronated B-ZSM-5 [18], allowed to obtain a titanium content higher than 2.5 wt%, but the catalytic activity of the resulting Ti-ZSM-5 was lower than that of hydrothermally synthesized TS-1 [19]. Therefore, many studies were performed on the improvement of the catalytic property of titanium silicalite [20] and the design of the reactor [21]. It was reported that modification by TPAOH could generate some mesopores, so that the diffusion limitation of substrates was reduced and the catalytic activity increased [22].

Small-crystal TS-1 with a crystal size of about  $600\text{ nm} \times 400\text{ nm} \times 250\text{ nm}$  exhibits a high catalytic activity in the hydroxylation of phenol [23], giving a phenol conversion of 22%. The high activity is attributed to the following factors: (a) small crystal size and large average pore diameter decrease the internal diffusion limitation and (b) large surface area and rough surface provide more active centers. In this contribution, we describe the treatment of small-crystal TS-1 with dilute organic base solutions of ethylamine (EA), diethylamine (DEA), tetramethyl ammonium hydroxide (TMAOH), tetrapropyl ammonium hydroxide (TPAOH) and tetrabutyl ammonium hydroxide (TBAOH) to further improve the catalytic activity of small-crystal TS-1, and to study the effect of bases on TS-1 and the reason for the improvement of activity.

## 2. Experimental

### 2.1. Synthesis and modification of TS-1

Small-crystal TS-1 was prepared in a hydrothermal system mentioned in Refs. [23,24], using colloidal silica (30 wt%) and titanium tetrachloride as silicon and titanium sources, respectively. TPABr was adopted as template and aqueous EA (65 wt%) as base. The mother liquor of nano-sized TS-1, which was used as crystallization seed, was prepared according to Ref. [25]. The molar composition of the gel was:

$$n(\text{SiO}_2) : n(\text{TiO}_2) : n(\text{TPABr}) : n(\text{EA}) : n(\text{H}_2\text{O}) = 1 : 0.02 : 0.15 : 1.5 : 25$$

$\text{TiCl}_4$  was added to isopropyl alcohol, and the obtained solution was mixed with colloidal silica. Finally, TPABr, EA, seed and water were gradually added to the colloidal silica. The resulting mixture was stirred for half an hour, then transferred to a Teflon lined autoclave and crystallized for 48 h at  $170^\circ\text{C}$ . The obtained solid was purified three times by precipitation method [24], followed by calcination at  $540^\circ\text{C}$  for 6 h.

The modification with base was carried out in a Teflon lined autoclave by keeping the as-synthesized small-crystal TS-1 and dilute organic base solution isothermal at  $170^\circ\text{C}$ , then washing and calcining the obtained powder at  $540^\circ\text{C}$  for 6 h. The modified samples were denoted as TS-1-X-C-T, while the X stood for the bases (EA, DEA, TMAOH, TPAOH and TBAOH), the C for the concentrations of bases (4, 6, 8 and 10 for 0.04, 0.06, 0.08 and 0.10 mol/L, respectively) and the T for the modification time (24, 36, 48, 60, 72 and 120 h). For example, the sample modified with 0.06 mol/L TPAOH solution for 48 h was denoted as TS-1-TPAOH-6-48. The unmodified sample was given TS-1-Null. For the sake of comparison, nano-sized TS-1 using the improved conventional method [26] was synthesized and given TS-1-Nano.

### 2.2. Characterization of TS-1

X-ray powder diffraction (XRD) patterns were measured on a Rigaku D/MAX-2400 using  $\text{Cu K}\alpha$  radiation. Fourier-transform

infrared (FTIR) spectra were recorded from  $4000$  to  $400\text{ cm}^{-1}$  on a Bruker EQUINOX55 spectrometer, and the KBr pellet technique was adopted. Ultraviolet–visible diffuse reflectance (UV–vis) spectra from 190 to 800 nm were obtained on a Jasco UV-550 spectrometer, and pure  $\text{BaSO}_4$  was used as reference. X-ray photoelectron spectra (XPS) were acquired with a Thermo VG ESCALAB250 instrument using  $\text{Al K}\alpha$  radiation and operating at a constant power of 260 W. The obtained spectra were analyzed by a curve-fitting program XPSPEAK, which was helpful for finding the best fitting results. A Perkin Elmer OPTIMA 2000DV Optical Emission Spectrometer provided the bulk element composition. Nitrogen physisorption was carried out on a Quantachrome AUTOSORB iQ2 physical sorption apparatus at 77 K. The surface area and pore volume were calculated according to the BET and DFT methods, respectively. The appearance of crystals was studied with a Hitachi S-4800 scanning electron microscope and a Tecnai G<sup>2</sup>20 S-Twin transmission electron microscope. *n*-Hexane and cyclohexane adsorption were carried out on a home-made physical sorption apparatus at room temperature.

### 2.3. Hydroxylation of phenol

The hydroxylation of phenol was carried out in a glass batch reactor. A total of 0.4 g modified small-crystal TS-1, 8.4 mL of acetone, 4.0 g of phenol and 30 wt%  $\text{H}_2\text{O}_2$  were added to the reactor. The molar ratio of phenol/ $\text{H}_2\text{O}_2$  was 3/1. The reaction was operated at  $80^\circ\text{C}$  for 6 h, and the residual  $\text{H}_2\text{O}_2$  was checked by iodometric titration. The products were analyzed on a Tianmei 7890F gas chromatograph with a FID and a SE-30 capillary column ( $30\text{ m} \times 0.25\text{ mm} \times 0.5\ \mu\text{m}$ ). The products were catechol (CAT), hydroquinone (HQ) and para-benzoquinone (PBQ). The conversion of  $\text{H}_2\text{O}_2$  ( $X(\text{H}_2\text{O}_2)$ ), conversion of phenol ( $X(\text{PHE})$ ), selectivity of CAT ( $S(\text{CAT})$ ), selectivity of HQ ( $S(\text{HQ})$ ), selectivity of PBQ ( $S(\text{PBQ})$ ) and utilization of  $\text{H}_2\text{O}_2$  ( $U(\text{H}_2\text{O}_2)$ ) were calculated as follows:

$$X(\text{H}_2\text{O}_2) = (n_0(\text{H}_2\text{O}_2) - n(\text{H}_2\text{O}_2))/n_0(\text{H}_2\text{O}_2)$$

$$X(\text{PHE}) = 1 - n(\text{PHE})/(n(\text{PHE}) + n(\text{CAT}) + n(\text{HQ}) + n(\text{PBQ}))$$

$$S(\text{CAT}) = n(\text{CAT})/(n(\text{CAT}) + n(\text{HQ}) + n(\text{PBQ}))$$

$$S(\text{HQ}) = n(\text{HQ})/(n(\text{CAT}) + n(\text{HQ}) + n(\text{PBQ}))$$

$$S(\text{PBQ}) = n(\text{PBQ})/(n(\text{CAT}) + n(\text{HQ}) + n(\text{PBQ}))$$

$$U(\text{H}_2\text{O}_2) = 3X(\text{PHE})/X(\text{H}_2\text{O}_2)$$

The  $n_0(\text{H}_2\text{O}_2)$  and  $n(\text{H}_2\text{O}_2)$  stand for the initial and final mole contents of  $\text{H}_2\text{O}_2$ , respectively. The  $n(\text{PHE})$ ,  $n(\text{CAT})$ ,  $n(\text{HQ})$  and  $n(\text{PBQ})$  represent the mole content of phenol, CAT, HQ and PBQ, respectively.

## 3. Results and discussion

### 3.1. Different organic bases

The XRD patterns of the small-crystal TS-1 modified with different bases are shown in Fig. 1. The five characteristic peaks of MFI topology at  $7.8^\circ$ ,  $8.8^\circ$ ,  $23.0^\circ$ ,  $23.9^\circ$  and  $24.4^\circ$  [27] changed slightly to higher  $2\theta$  after modification with TBAOH, which was considered to be due to recrystallization from a different crystal plane. The relative crystallinity (RC), which was calculated by comparing the total intensity of the five characteristic peaks with that of each sample and chose the highest total intensity as 100%, showed differences. Treated with base can cause the dissolution of silica [28],

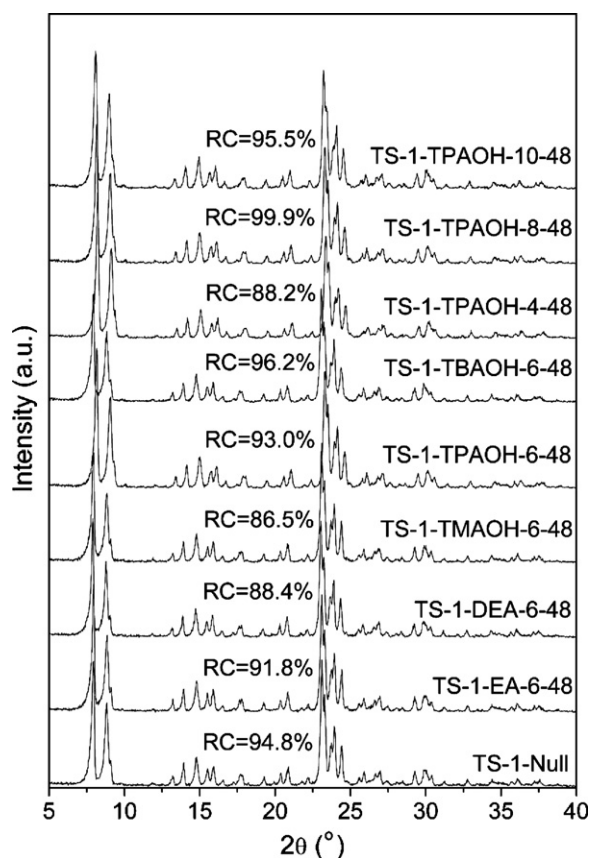


**Fig. 1.** XRD patterns of small-crystal TS-1 modified with different bases. RC stands for relative crystallinity.

and the dissolved silica might recrystallize in the presence of template, such as TPAOH [29]. There is a balance between dissolution and recrystallization. If the rate of dissolution is faster than that of recrystallization, the crystallinity will decrease, and vice versa. Therefore, the crystallinity usually decreases slightly after treating with dilute TPAOH solution [22]. If no template was present in the treating system or if the template was the structure-directing agent for another topology, the dissolved amorphous silica had difficulty to recrystallize or form another topology, leading to a lower crystallinity. The highest relative crystallinity was obtained for TS-1-TBAOH-6-48 and it was even a little higher than for TS-1-Null. TBAOH can be used as the template for MEL topology [30], the characteristic peaks of which are almost the same as those of MFI topology except that there is no diffraction peak at  $24.4^\circ$ . The strong structure-directing effect and basicity led to a faster

crystallization rate than dissolution rate of silica, and, as a consequence, the crystallinity of TS-1-TBAOH-6-48 was slightly higher than that of TS-1-Null. The increasing crystal size might be another factor responsible for the high crystallinity (cf. TEM images). EA and TPAOH are the templates for MFI topology, but the basicity and structure-directing effect of EA are both weaker than those of TPAOH, thus, the crystallinity of TS-1-EA-6-48 and TS-1-TPAOH-6-48 decreased slightly, and the former was lower than the latter. DEA can be used as the template for chabazite topology (such as SAPO-34) [31], while TMAOH is the template for sodalite topology (such as SAPO-20) [32], and they cannot structure-direct the synthesis of the MFI topology [33]. Therefore, the relative crystallinity, calculated according to the characteristic peaks of MFI, of TS-1-DEA-6-48 and TS-1-TMAOH-6-48 decreased.

The FTIR spectra of the samples are shown in Fig. 2(a). The weak band at  $870\text{ cm}^{-1}$  in TS-1-Null, which was assigned to the Si–OH group [34], disappeared in the modified samples. This may be the reason for the improvement of propene oxide selectivity in the epoxidation of propene [35]. A very weak band at  $870\text{ cm}^{-1}$  was present in the spectrum of TS-1-TMAOH-6-48, which may be due to the fact that the rate of recrystallization for TS-1-TMAOH-6-48 was so slow that more Si–OH became exposed. The band at  $960\text{ cm}^{-1}$  is due to the stretching vibration of  $[\text{SiO}_4]$  units, strongly influenced by titanium ions in neighboring coordination sites [36]. The intensity of this band is related to the strength of the Si–O–Ti bond and the content of titanium in the framework. It is obvious that the intensity increased after modification, due to the increasing strength of the Si–O–Ti bond and the clearance of channels exposing more framework Ti.

The UV–vis spectra of the six samples are shown in Fig. 2(b). The three major bands in the spectra, which are situated at 200–210 nm, 240–260 nm and 300–310 nm, are assigned to tetrahedrally coordinated Ti, a charge transfer process in isolated  $[\text{TiO}_4]$  or  $[\text{HOTiO}_3]$  units (usually called extra-framework Ti) and anatase  $\text{TiO}_2$ , respectively [37,38]. Obviously, the amount of anatase  $\text{TiO}_2$  increased to different extent after modification with different bases. The dissolution of silica in the treatment caused the loss of neighboring titanium, and the removed Ti can generate  $\text{TiO}_2$  or be reinserted into the framework, so that the amount of  $\text{TiO}_2$  increased. However, the  $\text{TiO}_2$  did not mainly originate from framework Ti, but also from extra-framework Ti, because the band at  $\sim 210\text{ nm}$  hardly changed while the band at  $\sim 240\text{ nm}$  clearly decreased. Extra-framework Ti and anatase  $\text{TiO}_2$  are considered to be inert in the oxidation reactions, thus, the transformation between them might not influence the catalytic activity.

The elemental analysis of the modified small-crystal TS-1 by ICP–AES for the bulk and by XPS for the surface is shown in Table 1. In the bulk, the molar Si/Ti ratio ( $n_B(\text{Si}/\text{Ti})$ ) of the modified samples were all lower than that on the unmodified sample, indicating that treating with bases led to a loss of silicon. Moreover, the  $n_B(\text{Si}/\text{Ti})$

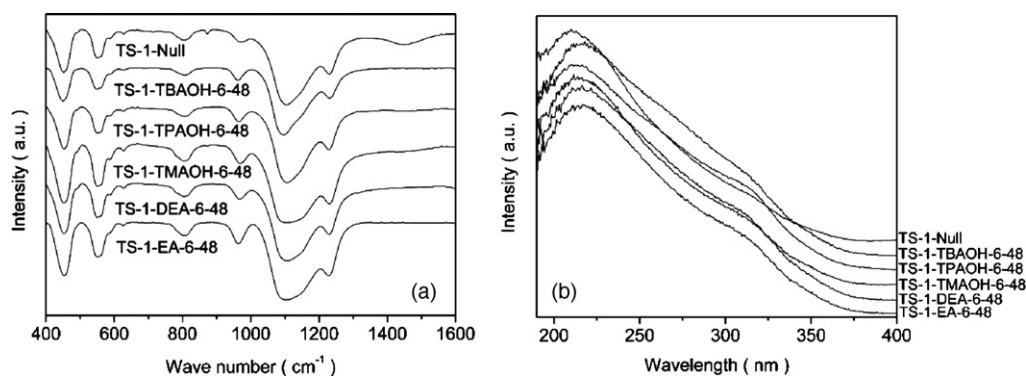


**Fig. 2.** FT-IR (a) and UV–vis (b) spectra of small-crystal TS-1 modified with different bases.

**Table 1**  
Elemental composition of modified small-crystal TS-1.

Samples	Si <sub>B</sub> (wt%) <sup>a</sup>	Ti <sub>B</sub> (wt%)	Al <sub>B</sub> (wt%)	Si <sub>S</sub> (wt%)	Ti <sub>S</sub> (wt%)	Al <sub>S</sub> (wt%)	n <sub>B</sub> (Si/Ti) <sup>b</sup>	n <sub>S</sub> (Si/Ti)	C <sub>F</sub> (%) <sup>c</sup>	C <sub>E</sub> (%)	C <sub>A</sub> (%)
TS-1-EA-6-48	44.97	2.04	0.12	44.92	1.02	0.69	37.79	75.61	64.0	14.5	21.5
TS-1-DEA-6-48	44.94	2.09	0.12	44.67	0.97	1.24	36.86	79.32	40.5	15.2	44.3
TS-1-TMAOH-6-48	44.96	2.04	0.14	44.79	0.99	0.91	37.78	77.56	85.0	7.8	7.2
TS-1-TPAOH-6-48	44.86	2.21	0.11	45.55	0.68	<0.01	34.80	114.18	58.1	19.9	22.0
TS-1-TBAOH-6-48	44.97	2.03	0.13	45.31	0.37	0.32	37.98	212.21	78.0	8.5	13.5
TS-1-Null	45.13	1.58	0.13	45.71	0.97	<0.01	48.97	80.57	76.8	12.4	10.8

<sup>a</sup> Si<sub>B</sub>, Ti<sub>B</sub> and Al<sub>B</sub> stand for the content of Si, Ti and Al in the bulk; Si<sub>S</sub>, Ti<sub>S</sub> and Al<sub>S</sub> stand for the content of Si, Ti and Al on the surface.

<sup>b</sup> n<sub>B</sub>(Si/Ti) and n<sub>S</sub>(Si/Ti) represent the molar ratio of Si/Ti in the bulk and on the surface, respectively.

<sup>c</sup> C<sub>F</sub>, C<sub>E</sub> and C<sub>A</sub> stand for the contents of framework Ti, extra-framework Ti and anatase TiO<sub>2</sub>, respectively.

of the modified samples were almost the same except for that of TS-1-TPAOH-6-48, due to the most loss of silicon. The content of aluminum stayed nearly constant in the treatment, because the insertion of aluminum into the framework is easy. The elemental surface composition was quite different from the bulk composition. The surface molar ratio of Si/Ti (n<sub>S</sub>(Si/Ti)) was higher than n<sub>B</sub>(Si/Ti) for the same sample, accounting for the fact that the surface of small-crystal TS-1 was rich of silicon. Furthermore, the n<sub>S</sub>(Si/Ti) for the samples treated with different bases were different. The values of TS-1-TPAOH-6-48 and TS-1-TBAOH-6-48 were much higher than the others, indicating that more recrystallization occurred on these two samples, and that TPA<sup>+</sup> and TBA<sup>+</sup> showed a protection effect on the Ti in the crystals (mainly framework Ti), so that the framework Ti remained in the crystals. The higher n<sub>S</sub>(Si/Ti) of TS-1-TBAOH-6-48 than of TS-1-TPAOH-6-48 may be due to the fact that more silica recrystallized on the surface, which was confirmed by XRD, so that more Ti on the surface was covered. However, the other bases did not have this ability, in other words, the framework Ti and Si dissolved together, and then recrystallized on the surface. Therefore, the n<sub>S</sub>(Si/Ti) of TS-1-EA-6-48, TS-1-DEA-6-48 and TS-1-TMAOH-6-48 were similar to that of TS-1-Null.

The Ti 2p photoelectron peaks for the samples are shown in Fig. 3. The Ti 2p<sub>3/2</sub> peaks were deconvoluted into three peaks. The two peaks at 460.3 eV and 458.7 eV are due to framework Ti and anatase TiO<sub>2</sub>, respectively [39–41]. The peak at 461.9 eV is assigned to isolated [TiO<sub>4</sub>] or [H<sub>2</sub>TiO<sub>3</sub>], corresponding to the band at ~240 nm in the UV–vis spectra. When the base could not protect the framework Ti, isolated [TiO<sub>4</sub>] would generate and cover the surface of the crystals, thus, the content of the peak at 461.9 eV would increase (see C<sub>E</sub> in Table 1), and the peak at 460.3 eV would shift to higher binding energy. If the isolated [TiO<sub>4</sub>] cannot recrystallize in time, it will generate anatase TiO<sub>2</sub>. When the base was strong, anatase TiO<sub>2</sub> was also easy to form, and the peak at 460.3 eV shifted to a lower binding energy.

Figs. 4 and 5 show the adsorption curves of respectively *n*-hexane and cyclohexane of the samples modified with different bases. *n*-Hexane can adsorb in the 8, 10 and 12-member ring channels of zeolites, while cyclohexane is too large to enter an 8-member ring channel, but may enter a channel with a 10-member or larger ring [42]. The diffusion of cyclohexane in 10-member ring channels is limited, but it can adsorb on the orifices. Therefore, the two adsorbates characterize different parts of TS-1 (10-member

ring). When the base can act as a template, a new framework will form, and *n*-hexane can be adsorbed in the new channels. Thus, the saturation adsorption amounts of *n*-hexane for different samples are almost the same, except for TS-1-DEA-6-48. The slightly lower adsorption amount of TS-1-DEA-6-48 is due to a lower crystallinity. The saturation adsorption amount of cyclohexane for TS-1-DEA-6-48 was the largest of all the samples, due to the generation of the largest amount of amorphous silica by treating with DEA, increasing the external surface area, on which cyclohexane could adsorb. The values of the other modified samples are smaller than that of the unmodified sample, because the recrystallization on the external surface and the generation of twin crystals enlarge the crystal size, which will decrease the external surface area relatively.

Fig. 6 shows the nitrogen physisorption isotherms of small-crystal TS-1. A hysteresis loop appears in each isotherm of modified sample, due to the generation of mesopores in the crystals. The BET surface areas of modified samples decrease after modification, except for TS-1-TPAOH-6-48 (see Table 2), due to the rapid recrystallization of silica and the generation of micropores for TS-1-TPAOH-6-48. The microporous surface area of TS-1-TPAOH-6-48 is much larger than those of the unmodified and other modified samples. The mesoporous volumes increase to different extent after modification with various bases. High catalytic activities are expected to be obtained over TS-1-TPAOH-6-48 and TS-1-TBAOH-6-48, due to the largest mesoporous volumes.

The TEM images of the modified samples are shown in Fig. 7. Irregular hollows appears in all the samples, which confirms the formation of hysteresis loops in N<sub>2</sub> physisorption isotherms. There is more amorphous silica and there are fewer hollows in the crystals of TS-1-EA-6-48 and TS-1-DEA-6-48 than in those of TS-1-TMAOH-6-48 and TS-1-TBAOH-6-48, due to the relative weaker basicity and structure-directing effect. The content of amorphous silica in TS-1-TBAOH-6-48 was very small, and the crystal size of TS-1-TBAOH-6-48 became larger, accompanied by the generation of twin crystals. Actually, silica was dissolved from the inside of the crystals, and then recrystallized from the external surface, forming twin crystals. Wang et al. reported that growth of a crystal ended of Si–OH groups, which were very active and ready to react with the other Si–OH groups to form Si–O–Si bond [43]. Therefore, the silica preferred to recrystallize along the Si–OH on the external surface. Different crystal planes have different energies. When the energy of a crystal plane matches that of the template, growth

**Table 2**  
Surface area and pore volume of modified small-crystal TS-1.<sup>a</sup>

Samples	A <sub>T</sub> (m <sup>2</sup> /g)	A <sub>Micro</sub> (m <sup>2</sup> /g)	V <sub>T</sub> (cm <sup>3</sup> /g)	V <sub>Micro</sub> (cm <sup>3</sup> /g)	V <sub>Meso</sub> (cm <sup>3</sup> /g)
TS-1-EA-6-48	440	337	0.36	0.15	0.21
TS-1-DEA-6-48	445	338	0.36	0.15	0.21
TS-1-TMAOH-6-48	432	312	0.35	0.15	0.20
TS-1-TPAOH-6-48	502	373	0.42	0.17	0.25
TS-1-TBAOH-6-48	445	306	0.41	0.16	0.25
TS-1-Null	453	334	0.32	0.15	0.17

<sup>a</sup> A<sub>T</sub> and A<sub>Micro</sub> stand for the total and microporous surface area, respectively. V<sub>T</sub>, V<sub>Micro</sub> and V<sub>Meso</sub> represent the total, microporous and mesoporous volumes, respectively.

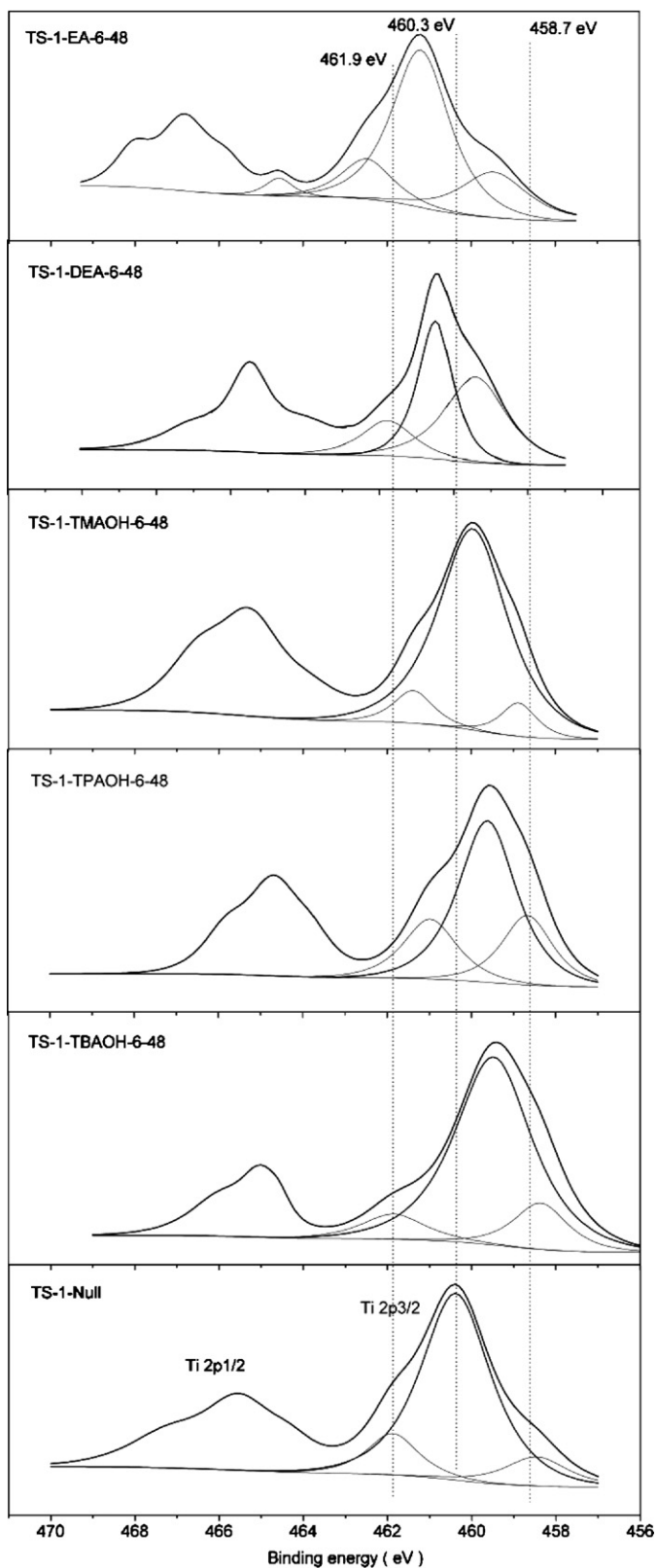


Fig. 3. XPS spectra of small-crystal TS-1 modified with different bases.

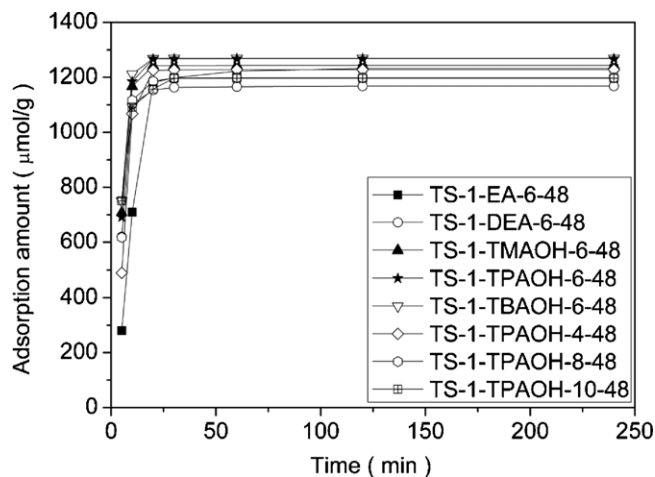


Fig. 4. *n*-Hexane adsorption of small-crystal TS-1 modified with different bases.

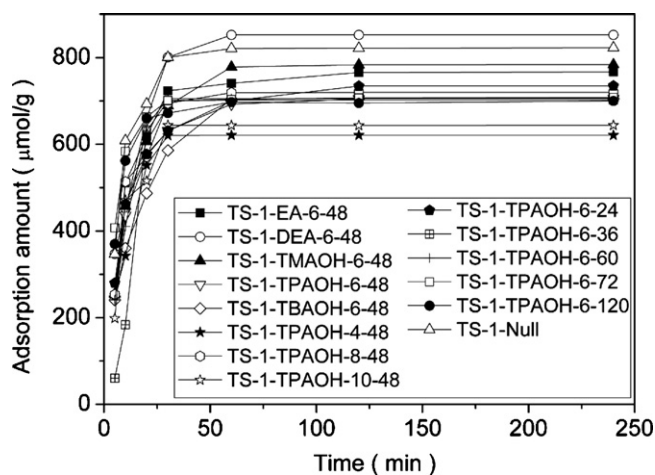


Fig. 5. Cyclohexane adsorption of small-crystal TS-1 modified with different bases.

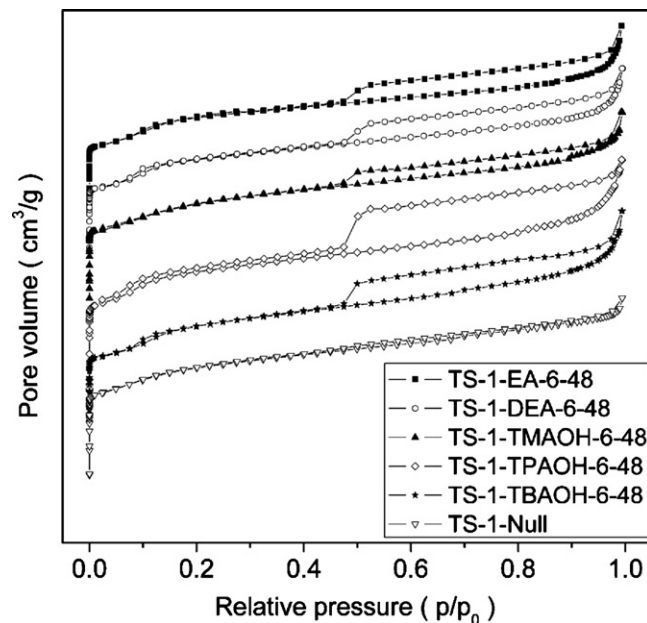


Fig. 6. Nitrogen physisorption isotherms of small-crystal TS-1 modified with different bases.

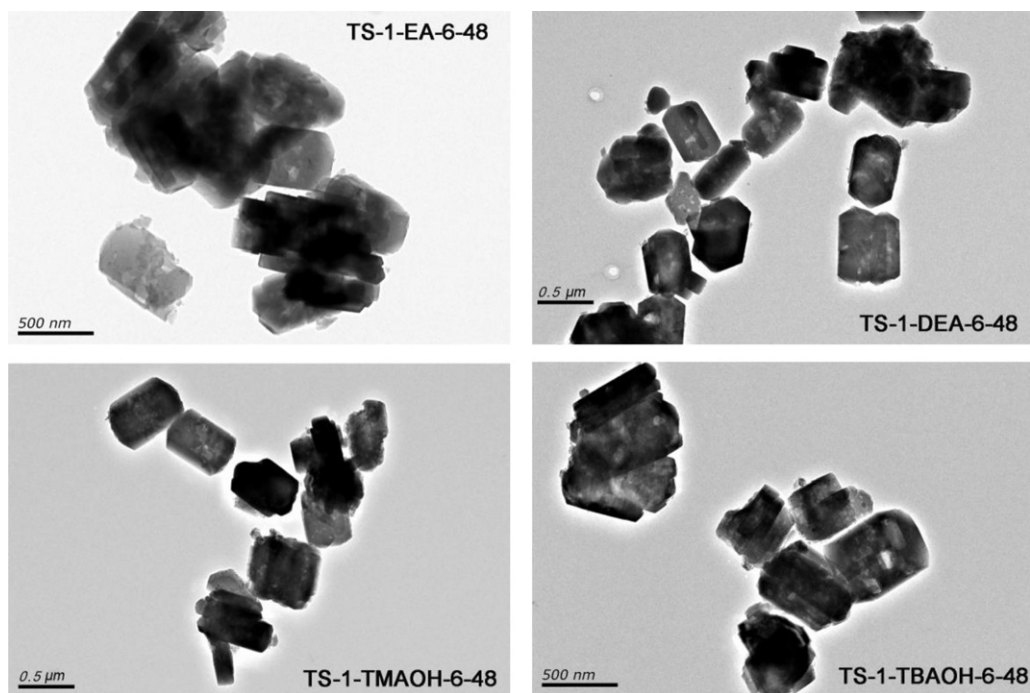


Fig. 7. TEM images of small-crystal TS-1 modified with different bases.

will occur. The characteristic peaks at  $2\theta$ -7.8°, 8.8°, 23.0° and 23.9° reflect the (0 1 1), (0 2 0), (5 0 1) and (3 0 3) planes, respectively [44]. The (0 2 0) plane of MFI topology is perpendicular to  $b$ -axis, which is the straight channel direction. The MEL topology only contains straight channels, so the energy of the (0 2 0) plane matches that of TBA<sup>+</sup>, thus, the recrystallization in TS-1-TBAOH-6-48 preferred to occur on the (0 2 0) plane. It was reported that a highly  $b$ -oriented TS-1 membrane showed a single peak at 8.8°, 17.8°, 26.8° and 36.0°, corresponding to the planes (0 2 0), (0 4 0), (0 6 0) and (0 8 0), respectively [45]. However, the XRD pattern of TS-1-TBAOH-6-48 showed a multiple-peak at 17.8°, due to the zigzag channel still existing in the TS-1. Face B in Chart 1 was considered to be rich in the (0 2 0) plane, thus, the recrystallization in TS-1-TBAOH-6-48 tended to occur on this face and generated a thicker crystal. When TPAOH was used to modify the small-crystal TS-1, recrystallization tended to occur along the  $a$ -axis, because the (1 0 0) plane, perpendicular to the  $a$ -axis, was the zigzag channel direction. Face A was rich in the (1 0 0) plane, so the crystal size of TS-1-TPAOH-6-48 was longer than those of the others.

The catalytic properties for hydroxylation of phenol over small-crystal TS-1 modified with different organic bases showed that the conversion of phenol increased after modification (Table 3), due to the elimination of diffusion limitation. The highest conversion of phenol was obtained over TS-1-TPAOH-6-48 and showed that the recrystallized structure had excellent catalytic activity. TS-2 (MEL topology), structure directed by TBAOH, also showed an activity for phenol hydroxylation, and the straight channels are beneficial for the diffusion of phenol and benzenediol, but the activity was lower than that of TS-1 [46]. Therefore, the selectivity of PBQ (the further oxidation product of HQ) for TS-1-TBAOH-6-48 was the lowest, but the conversion of phenol was lower than that of TS-1-TPAOH-6-48. Most of the framework Ti existed in the crystals, according to the XPS data. The generation of the hollows in the crystals made it easier for reactants to get in touch with the active centers. Although the  $n_S(\text{Si}/\text{Ti})$  in TS-1-TPAOH-6-48 and TS-1-TBAOH-6-48 were much higher than those in the other samples, the catalytic activity was not lower for these two samples, demonstrating that most reactions occurred in the channels of TS-1.

### 3.2. Different concentrations of TPAOH

The XRD patterns and relative crystallinity of small-crystal TS-1 modified with different concentrations of TPAOH solution are shown in Fig. 1. When the concentration was low (0.04 mol/L), the dissolved amorphous silica could not recrystallize rapidly, due to the insufficient availability of TPA<sup>+</sup> template. Thus, the relative crystallinity was very low. Along with the increase of the concentration, the amount of template increases, leading to an increase in relative crystallinity. When the concentration was 0.08 mol/L, the crystallinity reached a maximum, because the rate of recrystallization was faster than that of dissolution. At higher concentrations, the content of OH<sup>-</sup> in the modification system increased, accelerating the dissolution of silica, thus, the crystallinity decreased.

The  $n$ -hexane adsorption curves did not show a clear influence of the concentration of TPAOH on the saturation adsorption amount of  $n$ -hexane (Fig. 4). The saturation adsorption amount of cyclohexane was always lower after modification with any concentration of TPAOH solution than before (Fig. 5), similar to the relative crystallinity. The increase of crystal size caused a decrease of external surface area, which was considered as the main factor for the low adsorption amount. The particle size decreased, and then increased with the increase of TPAOH concentration (cf. the SEM and TEM images). Thus, the saturation adsorption amount increased, and then decreased.

The appearance of small-crystal TS-1 modified with different concentration of TPAOH is shown in Fig. 8. Much amorphous silica can be seen in the SEM image of TS-1-TPAOH-4-48, while it is not obvious in the other samples, leading to the lowest relative crystallinity for TS-1-TPAOH-4-48. Moreover, the  $a$ -oriented recrystallization grew to different length after modification, which was 730, 650, 700 and 730 nm for TS-1-TPAOH-4-48, TS-1-TPAOH-6-48, TS-1-TPAOH-8-48 and TS-1-TPAOH-10-48, respectively. When the concentration of TPAOH was low (0.04 mol/L), recrystallization needed to occur on the external surface of TS-1 crystals by using the surface as seeds [47,48], enlarging the crystal size. Increasing the concentration, TPA<sup>+</sup> could structure-direct the synthesis of new crystals, thus, the size decreased. When the

**Table 3**  
Catalytic properties of phenol hydroxylation over modified small-crystal TS-1.<sup>a</sup>

Samples	X(H <sub>2</sub> O <sub>2</sub> ) (%)	X(PHE) (%)	S(CAT) (%)	S(HQ) (%)	S(PBQ) (%)	U(H <sub>2</sub> O <sub>2</sub> ) (%)
TS-1-EA-6-48	99.4	27.4	43.3	54.7	2.0	88.0
TS-1-DEA-6-48	99.9	26.7	44.5	52.7	2.8	80.2
TS-1-TMAOH-6-48	99.5	27.4	47.3	50.2	2.5	82.6
TS-1-TPAOH-6-48	97.4	29.9	54.7	38.8	6.5	92.1
TS-1-TBAOH-6-48	99.7	28.0	54.2	43.9	1.9	84.3
TS-1-Null	97.0	22.1	53.4	43.4	4.2	68.4
TS-1-TPAOH-4-48	97.0	27.7	55.3	33.6	11.1	85.7
TS-1-TPAOH-8-48	97.5	28.6	54.3	34.4	11.2	88.0
TS-1-TPAOH-10-48	97.5	28.1	54.0	35.3	10.7	86.5
TS-1-TPAOH-6-24	97.3	24.7	53.4	37.3	9.3	76.2
TS-1-TPAOH-6-36	97.5	27.5	51.8	37.4	10.8	84.6
TS-1-TPAOH-6-60	97.5	31.4	54.3	38.9	6.8	96.6
TS-1-TPAOH-6-72	98.3	32.6	54.1	39.2	6.7	99.5
TS-1-TPAOH-6-120	98.3	32.6	56.1	39.3	4.6	99.5
TS-1-Nano	98.8	23.0	47.1	44.1	8.8	69.8

<sup>a</sup> Reaction conditions: catalyst 0.4 g, acetone 8.4 mL,  $n(\text{PHE})/n(\text{H}_2\text{O}_2)=3$ , phenol 4.0 g, 80 °C, 6 h.

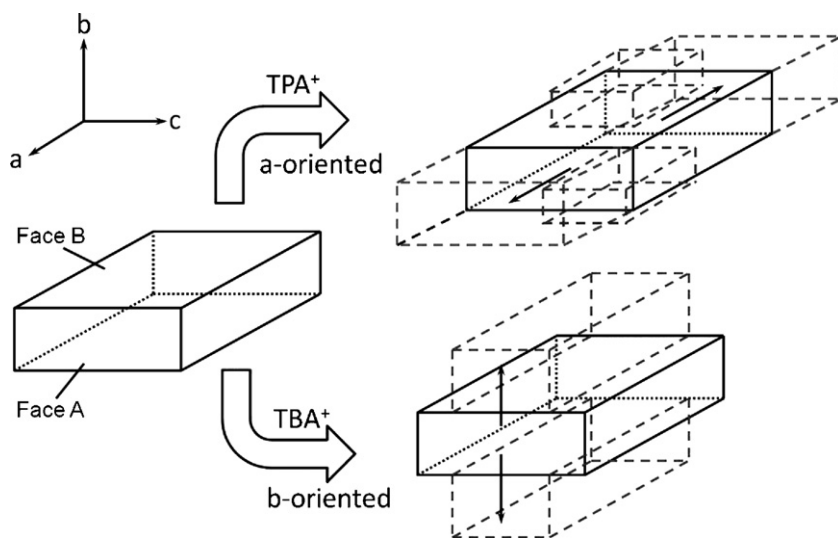


**Chart 1.** Recrystallization in the presence of TPA<sup>+</sup> and TBA<sup>+</sup>.

concentration was further increased, the basicity increased, leaching more silica and leading to a shortage of dissociative template in the solution. As a consequence, the recrystallization needed to occur on the external surface again, so that the size of crystal increased. Unlike the samples modified with other bases, few twin

crystals were observed in the samples treated with TPAOH, because the energy of the (1 0 0) plane was preferable with TPA<sup>+</sup>-structure-directed growth.

The catalytic properties of phenol hydroxylation over small-crystal TS-1 were improved after modification (Table 3). The

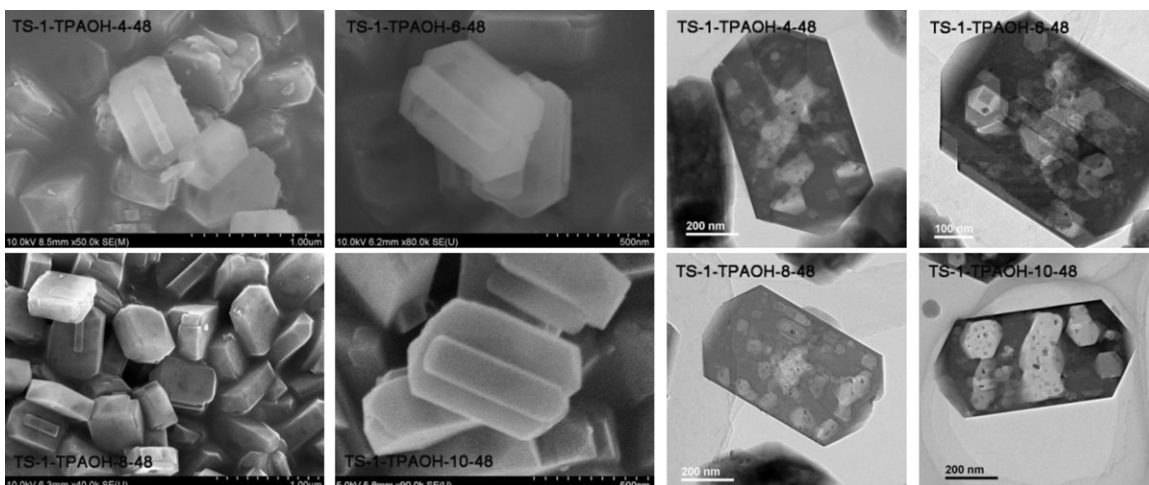


**Fig. 8.** SEM and TEM images of the modified small-crystal TS-1 with different concentrations of TPAOH solution.

highest conversion of phenol was obtained over TS-1-TPAOH-6-48, due to the smallest crystal size, the higher crystallinity and larger surface area. The smallest crystal size of TS-1-TPAOH-6-48 also led to the lowest selectivity of PBQ, due to the shortest channels.

### 3.3. Different modification time of TPAOH

The cyclohexane adsorption curves of the six samples are almost the same, except TS-1-TPAOH-6-24 (Fig. 5), and the saturation adsorption amount of each sample is less than that of TS-1-Null, due to the increasing crystal size.

The catalytic properties of phenol hydroxylation over small-crystal TS-1 modified with different times are shown in Table 3. With the increase of modification time, the conversion of phenol increased, until modified for 72 h, and then it stayed constant. When the modification time increased, the amount of dissolution of silica increased, so that more hollows were generated in the crystals, thus, the diffusion limitation of the reactants decreased and the conversion of phenol increased. However, the dissolution could not last endlessly, due to the protection effect of the TPA<sup>+</sup> template [49], in other words, the dissolution caused by TPAOH could not occur beside the framework Ti. When the TS-1 was modified for 72 h, the dissolution was considered to cease, leading to a stop in the recrystallization. Therefore, the properties for samples which were modified for more than 72 h were almost the same.

## 4. Conclusions

Modification of small-crystal TS-1 with different organic bases is a process of partly dissolution and partly recrystallization. Using TPAOH to modify the TS-1, the recrystallization preferred to occur *a*-oriented, while using TBAOH, it was *b*-oriented. TPA<sup>+</sup> and TBA<sup>+</sup> showed a protection effect on the framework Ti in the crystal.

The modification can improve the catalytic activity for the hydroxylation of phenol, due to the generation of hollows in the TS-1 crystals, decreasing the diffusion limitation of substrates. Most of the reactions occurred in the crystals, but not on the external surface. When 0.06 mol/L TPAOH was used to modify the TS-1 for 72 h, the conversion of phenol reached 32.6%, close to the theoretical conversion (33.3%).

## Acknowledgements

This work was financially supported by the program for New Century Excellent Talent in University (Grant NCET-04-0268) and the Plan 111 Project of the Ministry of Education of China. The authors also thank Prof. Roel Prins for his thoughtful discussion.

## References

- [1] M. Taramasso, G. Pergo, B. Notari, US Patent 4 410 501 (1983).
- [2] D.R.C. Huybrechts, L. De Bruycker, P.A. Jacobs, *Nature* 345 (1990) 240–242.
- [3] M.G. Clerici, G. Bellussi, U. Romano, *J. Catal.* 129 (1991) 159–167.
- [4] J.A. Martens, P. Buskens, P.A. Jacobs, A. van der Pol, J.H.C. van Hooff, C. Ferrini, H.W. Kouwenhoven, P.J. Kooyman, H. van Bekkum, *Appl. Catal. A: Gen.* 99 (1993) 71–84.
- [5] M.A. Mantegazza, G. Leofanti, G. Petrini, M. Padovan, A. Zecchina, S. Bordiga, *Stud. Surf. Sci. Catal.* 82 (1994) 541–550.
- [6] P. Wu, T. Komatsu, T. Yashima, *J. Phys. Chem. B* 102 (1998) 9297–9303.
- [7] U. Wilkenhöner, G. Langhendries, F. van Laar, G.V. Baron, D.W. Gammon, P.A. Jacobs, E. van Steen, *J. Catal.* 203 (2001) 201–212.
- [8] F.S. Xiao, Y. Han, Y. Yu, X.J. Meng, M. Yang, S. Wu, *J. Am. Chem. Soc.* 124 (2002) 888–889.
- [9] K. Weissermel, H.J. Arpe, *Industrial Organic Chemistry*, VCH, Weinheim, 1993, pp. 391–395.
- [10] S.F. Garcia, P.B. Weisz, *J. Catal.* 121 (1990) 294–311.
- [11] U. Romano, A. Esposito, F. Maspero, C. Neri, M.G. Clerici, *Stud. Surf. Sci. Catal.* 55 (1990) 33–41.
- [12] E. Duppey, P. Beaunier, A. Springuel-Huet, F. Bozon-Verduraz, J. Fraissard, J.M. Manoli, J.M. Brégeault, *J. Catal.* 165 (1997) 22–32.
- [13] C.W. Yoon, K.F. Hirsekorn, M.L. Neidig, X.Z. Yang, T.D. Tilley, *ACS Catal.* 1 (2011) 1665–1678.
- [14] D.H. Olson, G.T. Kokotailo, S.L. Lawton, W.M. Meier, *J. Phys. Chem.* 85 (1981) 2238–2243.
- [15] R. Millini, E. Previde Massara, G. Perego, G. Bellussi, *J. Catal.* 137 (1992) 497–503.
- [16] W.B. Fan, R.G. Duan, T. Yokoi, P. Wu, Y. Kubota, T. Tatsumi, *J. Am. Chem. Soc.* 130 (2008) 10150–10164.
- [17] P. Fejes, J.B. Nagy, J. Halász, A. Oszkó, *Appl. Catal. A: Gen.* 175 (1998) 89–104.
- [18] J. Gao, M. Liu, X.W. Guo, X.S. Wang, *Ind. Eng. Chem. Res.* 49 (2010) 2194–2199.
- [19] R.B. Quincy, M. Houalla, D.M. Hercules, *J. Catal.* 106 (1987) 85–92.
- [20] C. Ferrini, H.W. Kouwenhoven, in: G. Centi, F. Trifiro (Eds.), *New Developments in Selective Oxidation*, Elsevier, Amsterdam, 1990, pp. 53–60.
- [21] K. Yube, M. Furuta, K. Mae, *Catal. Today* 125 (2007) 56–63.
- [22] J.B. Mao, M. Liu, P. Li, X.S. Wang, *The 15th International Zeolite Conference*, Beijing, China, August 12–17, 2007.
- [23] Y. Zuo, X.S. Wang, X.W. Guo, *Ind. Eng. Chem. Res.* 50 (2011) 8485–8491.
- [24] Y. Zuo, X.S. Wang, X.W. Guo, *Microporous Mesoporous Mater.* 162 (2012) 105–114.
- [25] L.Q. Wang, X.S. Wang, X.W. Guo, *Chin. J. Catal.* 22 (2001) 513–514.
- [26] A. Thangaraj, S. Sivasanker, *J. Chem. Soc., Chem. Commun.* 2 (1992) 123–124.
- [27] G.N. Vayssilov, *Catal. Rev.-Sci. Eng.* 39 (1997) 209–251.
- [28] Y.R. Wang, A. Tuel, *Microporous Mesoporous Mater.* 113 (2008) 286–295.
- [29] Y.R. Wang, M. Lin, A. Tuel, *Microporous Mesoporous Mater.* 102 (2007) 80–85.
- [30] K.J.A. Raj, E.J.R. Malar, V.R. Vijayaraghavan, *J. Mol. Catal. A: Chem.* 243 (2006) 99–105.
- [31] G.Y. Liu, P. Tian, J.Z. Li, D.Z. Zhang, Z. Fan, Z.M. Liu, *Microporous Mesoporous Mater.* 111 (2008) 143–149.
- [32] H.Y. Li, J. Liang, Z.M. Liu, S.Q. Zhao, R.H. Wang, *Chin. J. Catal.* 9 (1988) 87–91.
- [33] G. Li, X.W. Guo, X.S. Wang, Q. Zhao, X.H. Bao, X.W. Han, L.W. Lin, *Appl. Catal. A: Gen.* 185 (1999) 11–18.
- [34] A.B. Bourlinos, S.R. Chowdhury, D.D. Jiang, Y.U. An, Q. Zhang, L.A. Archer, E.P. Giannelis, *Small* 1 (2005) 80–82.
- [35] S.T. Tsai, P.Y. Chao, T.C. Tsai, I. Wang, X.X. Liu, X.W. Guo, *Catal. Today* 148 (2009) 174–178.
- [36] D. Scarano, C. Zecchina, S. Bordiga, F. Geobaldo, G. Spoto, G. Petrini, G. Leofanti, M. Padovan, G. Tozzola, *J. Chem. Soc., Faraday Trans.* 89 (1993) 4123–4130.
- [37] E. Jorda, A. Tuel, R. Teissier, J. Kervennal, *Zeolites* 19 (1997) 238–245.
- [38] C. Perego, A. Carati, P. Ingallina, M.A. Mantegazza, G. Bellussi, *Appl. Catal. A: Gen.* 221 (2001) 63–72.
- [39] S. Vetter, G. Schulz-Ekloff, K. Kulawik, N.I. Jaeger, *Chem. Eng. Technol.* 17 (1994) 348–353.
- [40] G. Lassaletta, A. Fernández, J.P. Espinós, A.R. González-Elipe, *J. Phys. Chem.* 99 (1995) 1484–1490.
- [41] S. Contarini, P.A.W. van der Heide, A.M. Prakash, L. Kevan, *J. Electron. Relat. Phenom.* 125 (2002) 25–33.
- [42] R. Szostak, in: B. Davis (Ed.), *Molecular Sieves: Principles of Synthesis and Identification*, Van Nostrand Reinhold, New York, 1989, p. 10.
- [43] Z.X. Wang, W.F. Yan, D.Y. Tian, X.J. Cao, J.H. Yu, R.R. Xu, *Acta Phys.-Chim. Sin.* 26 (2010) 2044–2048.
- [44] M.M.J. Treacy, J.B. Higgins, *Collection of Simulated XRD Powder Patterns for Zeolites*, fifth ed., Elsevier, Amsterdam, 2007, p. 276.
- [45] X.M. Li, Y.S. Yan, Z.B. Wang, *Ind. Eng. Chem. Res.* 49 (2010) 5933–5938.
- [46] J.S. Reddy, S. Sivasanker, P. Ratnasamy, *J. Mol. Catal.* 71 (1992) 373–381.
- [47] J.W. Song, L. Dai, Y.Y. Ji, F.S. Xiao, *Chem. Mater.* 18 (2006) 2775–2777.
- [48] Z.F. Wu, J.W. Song, L.M. Ren, Y.Y. Ji, J.X. Li, F.S. Xiao, *Chem. Mater.* 20 (2008) 357–359.
- [49] J. Pérez-Ramírez, D. Verboekend, A. Bonilla, S. Abelló, *Adv. Funct. Mater.* 19 (2009) 3972–3979.